DOI: 10.61782/fa.2025.0098

FORUM ACUSTICUM
EURONOISE 2025

ACTIVE STRUCTURAL ACOUSTIC CONTROL (ASAC) FOR VIBRATING PLATES WITH OPENINGS IN VIBRO-ACOUSTIC SYSTEMS

Khaled Said Ahmed Maamoun[1,2*] **Stanislaw Wrona** [1] **Marek Pawelczyk**[1]
Hamid Reza Karimi[2]
[1] Department of Measurements and Control Systems, Silesian University of Technology, Gliwice, Poland
[2] Department of Mechanical Engineering, Politecnico di Milano, Milan, Italy

ABSTRACT

Active Structural Acoustic Control (ASAC) is a well-established technique for managing noise and vibration in vibro-acoustic systems. This study investigates the application of ASAC to vibrating plates with corner openings, a configuration that presents unique challenges due to localized stress concentrations and complex vibro-acoustic coupling. The placement and configuration of inertial actuators, which are integral to ASAC systems, are experimentally analyzed to optimize performance. The results show that the position of the opening significantly influences the overall system response, making the placement of inertial actuators unique to each configuration. Changing the location of the opening alters the vibrational and acoustic characteristics of the plate, requiring a tailored actuator arrangement for effective control. For fully clamped plates, placing actuators near the edges reduces their effectiveness in suppressing sound due to the high stress concentrations and limited vibrational energy at these regions. Additionally, positioning actuators around the openings introduces greater instability and nonlinearities into the system, further complicating the control dynamics. These findings highlight the necessity of considering both the opening location and actuator placement to optimize performance in vibro-acoustic systems.

Keywords: *active noise control, active structure acoustic control, vibro-acoustic systems, noise reduction.*

**Corresponding author: Khaled.maamoun@polsl.pl.*

1. INTRODUCTION

Openings in plate structures play a vital role in numerous engineering applications, particularly in vibro-acoustic coupled systems. These structures are widely employed across various domains, including household appliances, manufacturing, and vehicle engineering [1]. The shape, location, and relative position of openings concerning the noise source in such systems significantly influence the system's sound power response. For systems where openings are located in high-stress areas of vibrating plates, such as plate corners, additional sound power resonances are expected. Therefore, special attention is required to effectively address these systems [2]. Different techniques are employed to improve sound reduction in such systems, including both passive and active control methods [3].

Active Structural Acoustic Control (ASAC) plays a crucial role in mitigating noise transmission in various engineering applications by actively controlling structural vibrations. When properly implemented, ASAC can not only attenuate noise in localized regions but also achieve global noise reduction [4, 5]. It is generally implemented using a combination of passive noise barriers, vibration actuators, sensors, and a control system, as outlined in [6]. ASAC mitigates noise transmission through a structure by actively controlling its vibrations.

The authors in [7] theoretically evaluated a radiation-mode-based ASAC system for an enclosure with vent openings. However, their study was limited to tonal disturbances and did not explore practical real-world applications. A feedforward ASAC algorithm was later implemented on the lining panels of an aircraft cabin using a low-cost microcontroller, achieving a tonal noise reduction of 23 dB [8]. In [9], the authors examined the effectiveness of a tonal ASAC strategy that employs an experimentally identified radiation matrix to regulate sound power radiation, demonstrating superior performance over conventional active vibration control methods. However, their study did not consider broadband excitation.

Despite these advancements, the existing literature indicates a notable research gap in ASAC applications for systems with openings compared to fully enclosed structures. This highlights the need for further investigation to enhance ASAC effectiveness in such configurations.

The filtered-x least-mean-square (FxLMS) algorithm is the most popular active control algorithm due to its stability and simple structure [10]. The reference signal to the controller is filtered through the model of the secondary path between the actuator and the error sensors, ensuring effective noise attenuation. More features and have been added to FxLMS to enhance its characteristics, such as the Leaky FxLMS that introduces a small leakage factor to prevent coefficient drift and instability, making it more robust in nonstationary environments [11]. The Normalized FxLMS (NFxLMS) algorithm adjusts the step size based on the filtered reference signal power, ensuring faster convergence and better stability in varying input conditions [12].

The selection of the inertial actuator location on vibrating plates is crucial, as it directly affects the control system's ability to reduce noise [13]. Various studies have addressed this placement problem. Some studies optimize actuator placement based on vibration response [14], while others incorporate radiated sound into the cost function [15, 16]. The main contributions of this paper are twofold: i) an analysis of ASAC's effectiveness in mitigating noise from vibro-acoustic systems with openings, and ii) an investigation into the optimal placement of inertial actuators on vibrating plates, specifically considering corner regions with high stress concentrations.

The reminder of the paper is organized as follows: Section 2 is introduction of the experimental setup. Section 3 presents the results and the discussion. Finally, the conclusion is presented in Section 4.

2. EXPERIMENTAL SETUP

The experimental setup is designed to provide flexibility in testing actuators at various positions. The test plate can be replaced to evaluate systems with openings located at different corners. The laboratory room measures 5.8 meters in length and 3.5 meters in width. While the walls are lined with sound-absorbing materials, the presence of equipment and other objects within the room gives it acoustic characteristics more representative of a typical real-world environment rather than those of a dedicated acoustic chamber. The setup comprises a rectangular steel plate mounted on a concrete enclosure containing a loudspeaker. The plate is composed of steel with a density $\rho = 7850\,\mathrm{kg/m^3}$, Young's modulus $E = 210 \times 10^9\,\mathrm{Pa}$. The dimensions of the plate are $a = 0.42\,\mathrm{m}$, $b = 0.39\,\mathrm{m}$, and $h = 0.001\,\mathrm{m}$, representing its length, width, and thickness, respectively. The loudspeaker generates a random, band-limited noise signal with a position fixed at (0.3 m, 0.1 m, -0.3 m) for all the considered configurations. The concrete enclosure offers substantial sound attenuation, ensuring that the majority of the acoustic energy exiting the enclosure propagates through the plate and the circular opening. The active control system employs three Beyerdynamic MM1 error microphones and three DAEX32EP-4 inertial actuators, as illustrated in Fig. 1.

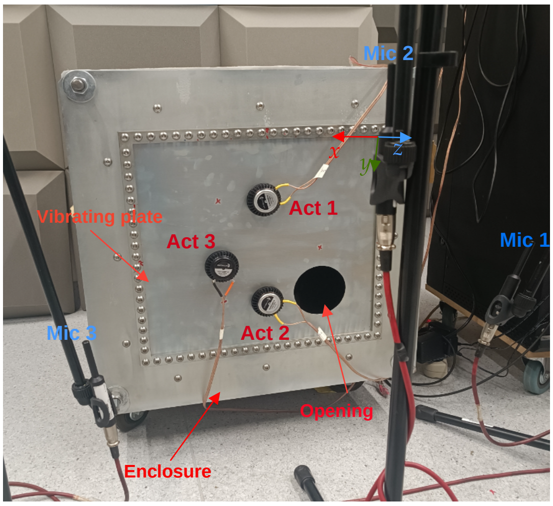

Figure 1: An overview of the experimental setup, showing a vibrating plate that contains a circular opening of a radius 0.05 m with center coordinates at (0.105 m, 0.265 m). Actuators (Act 1, Act 2, and Act 3) are mounted on the plate at (0.2 m, 0.1 m), (0.27 m, 0.2 m), and (0.2, 0.295 m), respectively. Microphones (Mic 1, Mic 2, and Mic 3) are positioned at the coordinates (-0.18 m, 0.12 m, 0.25 m), (0.21 m, -0.1 m, 0.4 m), and (0.53 m, 0.24 m, 0.25 m), respectively.

2.1 Algorithm

For active control, a feedforward multichannel FxLMS algorithm with a leakage factor is employed due to its simplicity and robustness [3], as illustrated in Fig. 2. The system normalizes based on the power of a single reference signal. The reference signal, denoted as $R(n)$, can be artificially generated or obtained via a reference microphone. The adaptive filter coefficients, represented by the vector W, consist of K elements generating the control signals $Y(n)$, while the canceling signals are given by $\hat{Y}(n)$.

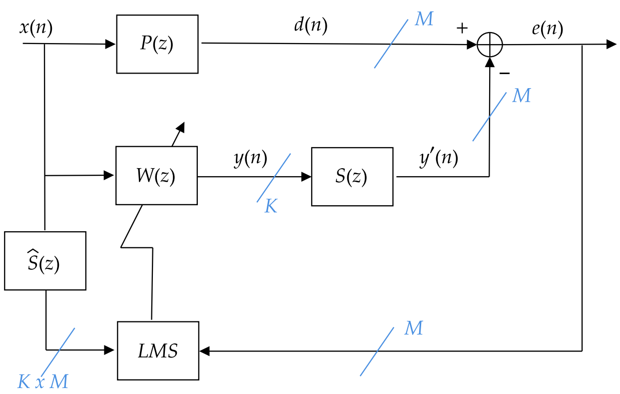

Figure 2: Block diagram of a single-reference multichannel feedforward FxLMS algorithm. M and K denote the number of outputs and secondary sources, respectively.

Since the secondary path matrix S is not directly available, it is approximated using an estimate $\hat{S}$. The $K \times M$ secondary paths are modeled as FIR filter impulse responses and adapted using the NLMS algorithm. The adaptive filter coefficients $W_k(n)$ are updated as:

$$W_k(n+1) = (1-\eta(n)\beta)W_k(n)+\eta(n)\sum_{m=1}^{M} R'_{km}(n)E_m(n), \tag{1}$$

where $R'_{km}(n)$ is the filtered reference signal, $E_m(n)$ is the error signal, and $\eta(n)$ is the normalized step size expressed as follows:

$$\eta(n) = \frac{\mu}{\sum_{k=1}^{K}\sum_{m=1}^{M} \|R'_{km}(n)\|^2}, \tag{2}$$

where μ is the fixed step size, $\|\cdot\|$ denotes the L^2-norm, and β is a leakage regularization factor.

In real-time operation, the total system latency from ADC input to DAC output is approximately 2.16 ms, which is close to the acceptable threshold for active control applications. This delay results from the combined effects of the output buffer (0.33 ms), the group delay introduced by IIR filters during downsampling (to 3 kHz) and upsampling (0.83 ms), and the inherent processing delay of the ADC and DAC at a 48 kHz sampling rate. The system is implemented using the Analog Devices SC598 with an SHARC+ core, integrated with the EVSOMCRR-EZKIT development board [17], featuring a 4-channel, 24-bit ADC and a 12-channel, 24-bit DAC.

3. RESULTS AND DISCUSSION

This study investigates the effect of actuator positioning on the performance of vibro-acoustic systems by evaluating four distinct actuator arrangements, as illustrated in Fig.3. The selected configurations are designed to reflect both critical and potentially optimal actuator placements, informed by the physical characteristics of the system [2, 15].

The mass of the actuators is approximately 140 g, which can alter the system's response even without control. Fig. 4 compares the power spectral density (PSD) of the three error microphones for the four configurations under consideration.

The difference between Configuration 1 and Configuration 4 is particularly noticeable in the frequency range between 150 Hz and 200 Hz. This is due to the fact that, in Configuration 4, the actuator masses are positioned near the edges of the clamped plate, regions of high stress, resulting in a higher sound power response.

In contrast, Configuration 1 places two of the three actuators closer to the opening, which helps to reduce vibrations in that region, thereby minimizing the radiated sound power. Moreover, Configurations 2 and 3 exhibit similar performance, as the actuators are more concentrated near the center of the plate. To assess the reduction achieved through active control, the four configurations are compared to the average microphone response in the absence of control. As shown in Fig. 5, ASAC effectively minimizes the system's sound power response, indicating that it is not only effective in reducing radiated sound but also in mitigating noise leakage through the opening. The actuator placement near the clamped edges in Configuration 4 restricts the system's ability to vibrate actively. The displacement is constrained, and this helps generate anti-noise waves that counteract sound leakage through

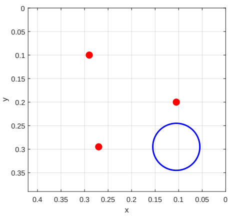

(a) Configuration 1.

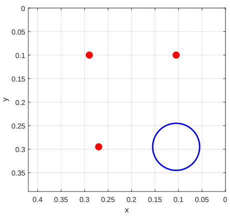

(b) Configuration 2.

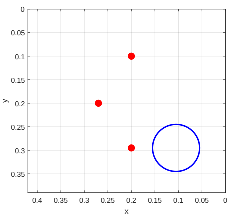

(c) Configuration 3.

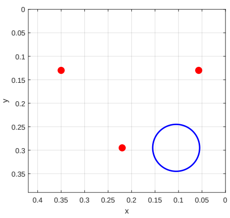

(d) Configuration 4.

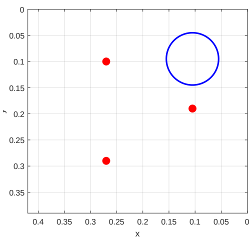

(e) Configuration 5.

Figure 3: An overview of the four configurations of the actuators' arrangements.

the opening.

Configuration 3 demonstrates the best performance across the considered frequency range. This is attributed to one actuator being positioned closer to the opening—allowing greater flexibility for displacement—combined with a central actuator arrangement that provides a balanced response across most mode shapes. Configurations 1 and 2 may be advantageous when targeting specific resonances. For instance, Configuration 2 positions the actuators closer to the anti-nodal regions of the third and fourth mode shapes of the rectangular plate [2], making it more effective in that frequency range.

To evaluate the influence of the relative position of the opening with respect to the excitation source, as well as the effect of actuator arrangement, Configuration 5 is tested and compared with Configuration 1. This comparison is considered fair, as both configurations share a similar actuator arrangement, as illustrated in Fig. 6.

Configuration 5 exhibits lower sound power levels compared to Configuration 4, particularly in the frequency range between 135 Hz and 200 Hz. This improvement is attributed to the fact that the opening in Configuration 5 is positioned farther from the internal noise source, resulting in reduced sound leakage through the opening. When ASAC is applied, Configuration 5 demonstrates enhanced control performance due to the revised opening location, which makes the actuator placement—particularly that of Act 1 and 3—more favorable for inducing effective vibrational displacement near the aperture. As a result, despite having the same actuator arrangement as Configuration 1, the system achieves over 5 dB additional noise reduction in the frequency ranges of 70–125 Hz and 170–200 Hz due to the relocated opening.

4. CONCLUSION

This study experimentally examined the application of Active Structural Acoustic Control (ASAC) in vibro-acoustic systems with structural openings, focusing on the influence of inertial actuator placement and opening location on control effectiveness. Five actuator configurations were evaluated on a fully clamped vibrating plate to assess how spatial arrangement and structural characteristics impact both passive and active noise control performance.

The results demonstrate that actuator positioning significantly affects the system's vibrational and acoustic response. Configurations with actuators placed near the clamped edges—regions of high stress and low vibrational energy—showed limited effectiveness in both passive damping and active control. In contrast, configurations with actuators distributed closer to the plate center or near the opening, such as Configuration 3, provided more balanced control across the frequency range, benefiting from greater displacement flexibility and improved mode shape engagement. Moreover, Configuration 5 revealed that relocating the opening farther from the noise source, even with the same actuator arrangement as Configuration 1, can lead to an additional 5 dB reduction in key frequency ranges. This highlights that the opening's position, in relation to the excitation source and actuators, plays a crucial role in minimizing sound leakage and enhancing ASAC performance.

These findings underscore the importance of tailoring

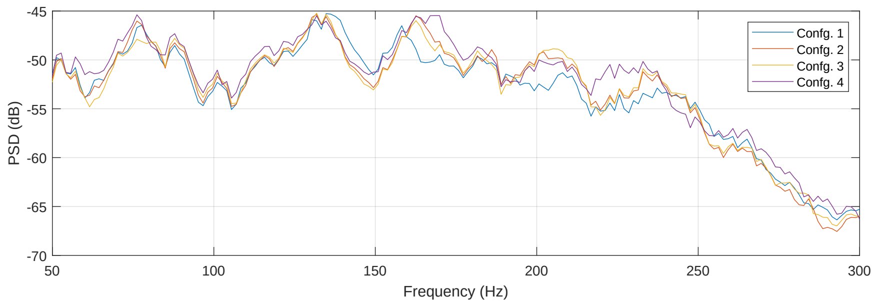

(a) Mic 1

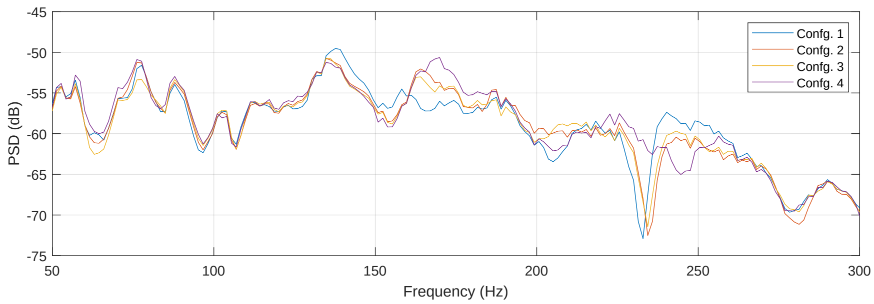

(b) Mic 2

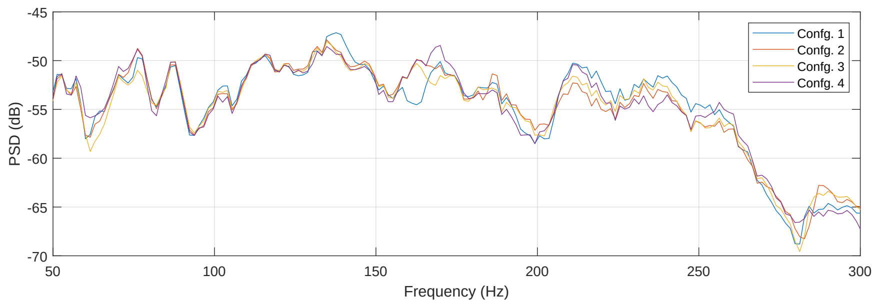

(c) Mic 3

Figure 4: PSD of the three error signals for the configurations without active control.

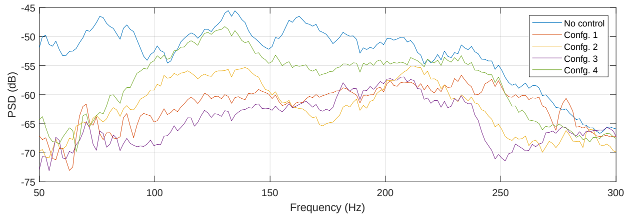

(a) Mic 1

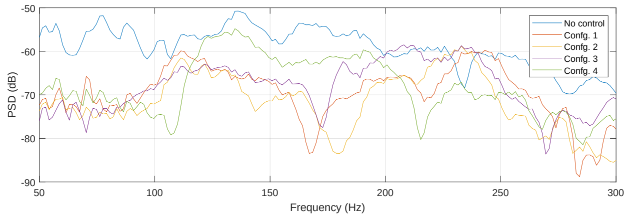

(b) Mic 2

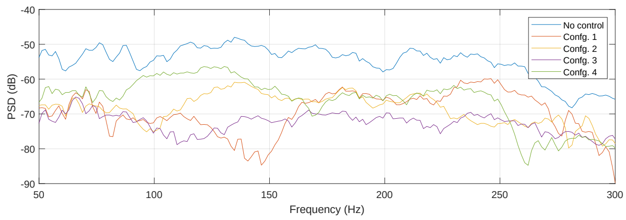

(c) Mic 3

Figure 5: PSD of the three error signals for the configurations with active control.

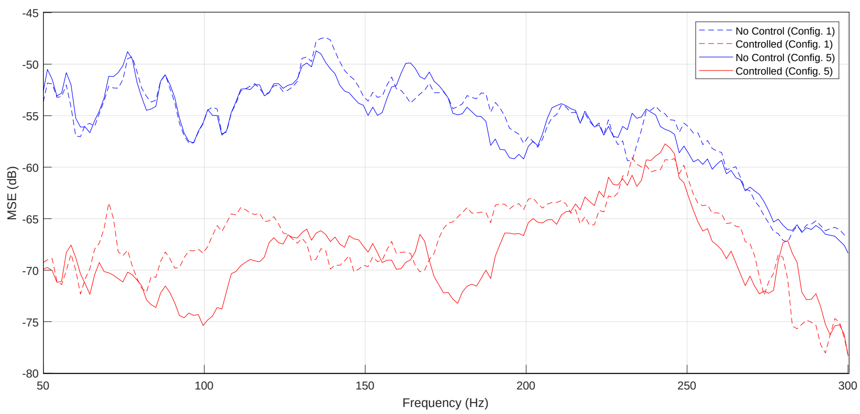

Figure 6: Mean square error (MSE) of the three error microphones signals for Configurations 1 and 5.

actuator placement strategies to the specific structural and acoustic context, particularly in systems with openings, to maximize control efficiency and achieve optimal noise reduction.

5. ACKNOWLEDGMENTS

The work was supported by the project IN-NOVA: Active reduction of noise transmitted into and from enclosures through encapsulated structures, which has received funding from the European Union's Horizon Europe program under the Marie Sklodowska-Curie grant agreement no. 101073037.

6. REFERENCES

[1] Z. Zhu, Y. Song, Y. Zhang, Q. Liu, and G. Wang, "Sound radiation of the plate with arbitrary holes," *International Journal of Mechanical Sciences*, vol. 264, p. 108814, 2024.

[2] K. S. A. Maamoun, S. Wrona, M. Pawelczyk, and H. R. Karimi, "Shaping of the frequency response of vibrating plates with openings for vibro-acoustic systems," *Mechanical Systems and Signal Processing*, vol. 218, p. 111539, 2024.

[3] S. Elliott, *Signal processing for active control*. Elsevier, 2001.

[4] K. Mazur, S. Wrona, and M. Pawelczyk, "Design and implementation of multichannel global active structural acoustic control for a device casing," *Mechanical Systems and Signal Processing*, vol. 98, pp. 877–889, 2018.

[5] A. Chraponska, S. Wrona, J. Rzepecki, K. Mazur, and M. Pawelczyk, "Active structural acoustic control of an active casing placed in a corner," *Applied Sciences*, vol. 9, no. 6, p. 1059, 2019.

[6] S. Wrona and M. Pawelczyk, "Active reduction of device narrowband noise by controlling vibration of its casing based on structural sensors," in *Proceedings of the 22nd International Congress on Sound and Vibration, Florence, Italy*, pp. 12–16, 2015.

[7] O. Jeon, H.-G. Kim, J. Kook, S. M. Kim, and S. Wang, "Active structural acoustic control for radiated sound power reduction of enclosure with vent holes based on radiation modes," *Journal of Mechanical Science and Technology*, vol. 36, no. 7, pp. 3313–3327, 2022.

[8] M. Misol, S. Algermissen, M. Rose, and H. P. Monner, "Aircraft lining panels with low-cost hardware for active noise reduction," in *2018 Joint Conference-Acoustics*, pp. 1–6, IEEE, 2018.

[9] J. Milton, J. Cheer, and S. Daley, "Active structural acoustic control using an experimentally identified radiation resistance matrix," *The Journal of the Acoustical Society of America*, vol. 147, no. 3, pp. 1459–1468, 2020.

[10] P. Song and H. Zhao, "Filtered-x least mean square/fourth (fxlms/f) algorithm for active noise control," *Mechanical Systems and Signal Processing*, vol. 120, pp. 69–82, 2019.

[11] O. Tobias and R. Seara, "Leaky-fxlms algorithm: stochastic analysis for gaussian data and secondary path modeling error," *IEEE Transactions on Speech and Audio Processing*, vol. 13, no. 6, pp. 1217–1230, 2005.

[12] M. T. Akhtar and W. Mitsuhashi, "A modified normalized fxlms algorithm for active control of impulsive noise," in *2010 18th European Signal Processing Conference*, pp. 1–5, 2010.

[13] X. Liu, G. Cai, F. Peng, and H. Zhang, "Piezoelectric actuator placement optimization and active vibration control of a membrane structure," *Acta Mechanica Solida Sinica*, vol. 31, pp. 66–79, 2018.

[14] D. Chhabra, G. Bhushan, and P. Chandna, "Optimal placement of piezoelectric actuators on plate structures for active vibration control via modified control matrix and singular value decomposition approach using modified heuristic genetic algorithm," *Mech. Adv. Mat. Struct.*, vol. 23, no. 3, pp. 272–280, 2016.

[15] S. Wrona, M. Pawelczyk, and J. Cheer, "Acoustic radiation-based optimization of the placement of actuators for active control of noise transmitted through plates," *Mechanical Systems and Signal Processing*, vol. 147, p. 107009, 2021.

[16] Q. Mao and S. Pietrzko, "Control of noise and structural vibration," *Cham, Switzerland: Springer, DOI*, 2013.

[17] Analog Devices, "ADSP-SC598 Product Page," 2025. Accessed: 2025-03-01.